ACS Catalysis

Subscriber access provided by STEPHEN F AUSTIN STATE UNIV

Article

Experimental and Theoretical Studies on Ru(II)-Catalyzed Oxidative C-H/C-H Coupling of Phenols with Aromatic Amides Using Air as Oxidant: Scope, Synthetic Applications and Mechanistic Insights

Luoqiang Zhang, Lei Zhu, Yuming Zhang, Yudong Yang, Yimin Wu, Weixin Ma, Yu Lan, and Jingsong You

ACS Catal., **Just Accepted Manuscript** • DOI: 10.1021/acscatal.8b02816 • Publication Date (Web): 06 Aug 2018

Downloaded from http://pubs.acs.org on August 6, 2018

Just Accepted

"Just Accepted" manuscripts have been peer-reviewed and accepted for publication. They are posted online prior to technical editing, formatting for publication and author proofing. The American Chemical Society provides "Just Accepted" as a service to the research community to expedite the dissemination of scientific material as soon as possible after acceptance. "Just Accepted" manuscripts appear in full in PDF format accompanied by an HTML abstract. "Just Accepted" manuscripts have been fully peer reviewed, but should not be considered the official version of record. They are citable by the Digital Object Identifier (DOI®). "Just Accepted" is an optional service offered to authors. Therefore, the "Just Accepted" Web site may not include all articles that will be published in the journal. After a manuscript is technically edited and formatted, it will be removed from the "Just Accepted" Web site and published as an ASAP article. Note that technical editing may introduce minor changes to the manuscript text and/or graphics which could affect content, and all legal disclaimers and ethical guidelines that apply to the journal pertain. ACS cannot be held responsible for errors or consequences arising from the use of information contained in these "Just Accepted" manuscripts.

ACS Publications

is published by the American Chemical Society. 1155 Sixteenth Street N.W., Washington, DC 20036

Published by American Chemical Society. Copyright © American Chemical Society. However, no copyright claim is made to original U.S. Government works, or works produced by employees of any Commonwealth realm Crown government in the course of their duties.

Experimental and Theoretical Studies on Ru(II)-Catalyzed Oxidative C–H/C–H Coupling of Phenols with Aromatic Amides Using Air as Oxidant: Scope, Synthetic Applications and Mechanistic Insights

Luoqiang Zhang,† Lei Zhu,‡ Yuming Zhang,† Yudong Yang,† Yimin Wu,† Weixin Ma,† Yu Lan,*,‡ and Jingsong You*,†

†Key Laboratory of Green Chemistry and Technology of Ministry of Education, College of Chemistry, Sichuan University, 29 Wangjiang Road, Chengdu 610064, PR China

‡School of Chemistry and Chemical Engineering, Chongqing University, Chongqing 400030, PR China

Supporting Information Placeholder

ABSTRACT: We herein illustrate the dual chelation-assisted strategy for a Ru(II)-catalyzed oxidative *ortho*-C–H/C–H cross-coupling of phenols with (hetero)aromatic amides with the aid of $Zn(OTf)_2$, which enables to rapidly assemble a rich library of 2'-hydroxybiphenyl-2-carboxylic acid derivatives. This protocol features broad substrate scope, excellent functional group tolerance, air as the terminal oxidant, low molar ratio of coupling partners and scale-up synthesis. Particularly, this methodology is tolerant of more complex natural product derivatives, thus providing an opportunity for late-stage functionalization. This protocol is also used as a key step for the concise synthesis of Palomid 529, a drug in development for the treatment of glioblastoma and neovascular age-related macular degeneration. With a combination of experimental and theoretical methods, we get more insight into the essential issues of strategy determining the reaction process. The stronger coordinating ability of 2-aryloxypyridine and the less steric hindrance of amide are pivotal to the high chemoselectivity of cross-coupling over homo-coupling. The first C–H bond activation step takes place at the amide substrate, and the following C–H bond activation at 2-aryloxypyridine is involved in the rate-determined step.

KEYWORDS: *C–H activation, ruthenium catalysis, oxidative C–H/C–H cross-coupling, dual chelation-assisted strategy, 2,2'-difunctional biaryl*

INTRODUCTION

In the past decade, transition metal-catalyzed oxidative Ar–H/Ar–H coupling reaction, in which two C–H activation processes are involved, is emerged as one of the most ideal strategies to synthetize diverse biaryls due to high atom- and step-economy.[1] In these reactions, a directing group is often assembled in one coupling partner to control the regioselectivity and enhance the reactivity.[1,2] In principle, the regioselectivity of both aromatic coupling partners could be controlled efficiently while both of the substrates bear a directing group ("dual chelation-assisted strategy").[3,4] The resulting 2,2'-difunctional biaryls are highly important scaffolds. 2,2'-Difunctional biaryls are found frequently in ligands for transition metal catalysis, pharmaceuticals, natural products, organic functional materials and are also versatile intermediates in organic synthesis.[5] Because the chelating functionalities containing sulphur, nitrogen and oxygen atoms enable to serve as the directing group, transition metal-catalyzed oxidative C–H/C–H cross-coupling between chelating functionality-bearing arenes would be a straightforward approach to access a large library of 2,2'-difunctional biaryls. Despite practical usefulness, it seems difficult to use and manipulate this strategy owing to persistent obstacles associated with the chemoselectivity control of cross-coupling over homo-coupling (Scheme 1a).[3] To date, the relevant examples are still very limited and appeared until 2015.[3g,4] Moreover, owing to inherent intricacies, the understanding of the dual chelation-assisted strategy is far from deep so far. Among these precedent works, a significant excess of either coupling partner (usually at least 3.0 equiv,[3g,,4a,4c-e] even up to 30 equiv[4e]) was typically required to ensure the output of the cross-coupled product. In an example, a 1:1 ratio of substrates even led to only 6% yield of cross-coupled product along with 65% yield of the homo-coupled product.[4d] In addition, these cross-coupling reactions also required a large amount of metal salts as the oxidant.[3g,4] Thus, the development of more effective reactions enabling to overcome the above limitations is in high demand. It is also strongly desired to get more insight into the essential issues of strategy determining the reaction process.

2'-Hydroxybiphenyl-2-carboxylic acid derivatives are important structural motifs in many natural products and pharmaceuticals,[6] such as ulocladol,[6a] 6'-hydroxy justicidin A,[6b] mongolicumin A,[6c] fissitungfines A,[6d] and Palomid 529[6e] (Scheme 2). Very recently, we reported a Rh-catalyzed oxidative C–H/C–H cross-coupling reactions between *N*-acylanilines and benzamides to forge 2-amino-2'-carboxybiaryl scaffolds.[7] Herein we wish to demonstrate an aerobic Ru(II)-catalyzed oxidative *ortho*-C–H/C–H cross-coupling between phenols and (hetero)aromatic amides through the dual

chelation-assisted strategy with the help of $Zn(OTf)_2$, which enables to rapidly synthesize the 2'-hydroxybiphenyl-2-carboxylic acid skeletons (Scheme 1b). Mechanistic studies reveal that the strong coordinating ability of 2-aryloxypyridine and the less steric hindrance of amide play a key role in determinating chemoselectivity, which would provide a guidance for the highly efficient synthesis of unsymmetrical 2,2'-difunctional biaryls.

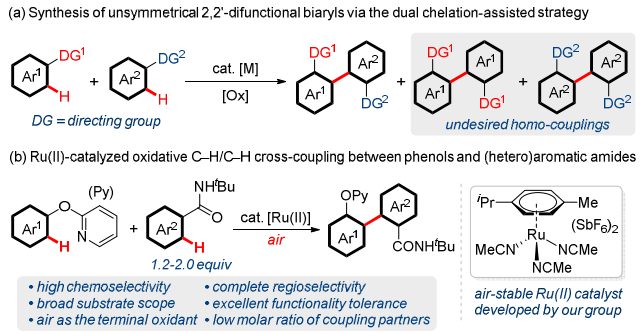

Scheme 1. Oxidative Ar–H/Ar–H cross-coupling reactions based on the dual chelation-assisted strategy

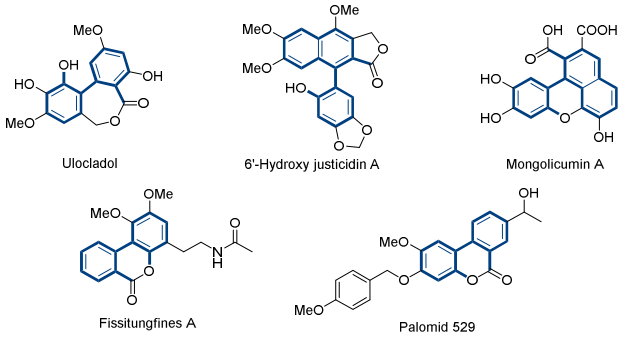

Scheme 2. Selected examples of 2'-hydroxybiphenyl-2-carboxylic acid derivatives

RESULTS AND DISCUSSION

Optimization of the Reaction Conditions. The ruthenium catalysts have the advantages such as low-cost metal precursors, easy preparation, and good stability. Thus, our investigation commenced with the exploitation of the matched directing group pair for the oxidative cross-coupling between phenols and benzoic acids under the ruthenium catalysis (Scheme 3). The results indicated that phenols with a strong coordinating group (aza-aromatics) and *N*-alkyl or *N*-phenyl-substituted benzamides would be a suitable combination. However, no cross-coupled product was detected when 6-methyl-2-pyridinyloxyl was used as the directing group of phenol, probably because of a large steric hindrance (**DG1b**). Phenols with oxime (**DG1e**) or oxyacetamide (**DG1f**) decomposed completely under the indicated conditions. Weakly coordinating groups like dimethylcarbamate **(DG1g)** and pivalate **(DG1h)** were ineffective directing groups. No desired product was observed in the attempts of acid (**DG2a**), ester (**DG2b**), free amide (**DG2c**), *N*-pivaloylamide (**DG2i**), and *N*-methoxyamide (**DG2j**). Finally, 2-pyridyloxyl (**DG1a**) and *N*-(*tert*-butyl) carbamyl (**DG2f**) were identified as a matched directing group pair for phenols and benzoic acids, respectively.

With the identified directing groups in hand, we focused on the optimization of the catalytic system (Table 1). 2-(*o*-Tolyloxy)pyridine **1a** and *N*-(*tert*-butyl)benzamide **2a** were selected as the model substrates. In the presence of $[Ru(p\text{-cymene})Cl_2]_2$ (2.5 mol%), $AgSbF_6$ (10 mol%), $Cu(OAc)_2$ (1.5 equiv) and AcOH (20 mol%) under air, the desired cross-coupled product **3a** was obtained in 11% yield along with 18% yield of the acetoxylated byproduct **1ab**,[8] 1% yield of the homo-coupled *N*-(*tert*-butyl)benzamide (**2aa**) and 62% recovery yield of unreacted **1a**. No homo-coupling of **1a** was detected (Table 1, entry 1). The structure of **3a** was confirmed by X-ray crystallography. The oxidants were next investigated. Considering easy availability, low cost and environmental friendliness of air or O_2,[9] we tried to conduct the reaction using air or O_2 as the oxidant (Table 1, entries 2-3). In the absence of a metal oxidant, **3a** could be obtained in 16% and 12% yields under an air or O_2 atmosphere, respectively. A combination of $Cu(OAc)_2$ (5 mol%) and air as the terminal oxidant delivered **3a** in 36% yield (Table 1, entry 4). Further reducing the amount of $Cu(OAc)_2$ to 3 mol% could slightly increase the yield of **3a** to 39% (Table 1, entry 5). No cross-coupling reaction occurred in the absence of $AgSbF_6$, indicating the essential role of cationic ruthenium(II) species in this transformation (Table 1, entry 6). Thus, $[Ru(p\text{-cymene})(MeCN)_3](SbF_6)_2$ (5 mol%), an air-stable cationic Ru(II) complex developed by our group,[10] was employed as the catalyst, giving a similar yield of **3a** under otherwise identical reaction conditions (Table 1, entry 7). The concentration of substrates was found to have a significant influence on the yield of **3a** and a higher concentration was identified to favor the cross-coupling reaction (Table 1, entries 8-9). Gratifyingly, the addition of $Zn(OTf)_2$ (20 mol%) could improve the yield of **3a** to 68% and significantly inhibit the undesired homo-coupling of **1a** (Table 1, entry 10). Further screening of reaction time (Table 1, entries 11-12) and substrate ratio (Table 1, entries 13-16) led to the optimized reaction conditions consisted of $[Ru(p\text{-cymene})(MeCN)_3](SbF_6)_2$ (5 mol%), $Cu(OAc)_2$ (3 mol%), $Zn(OTf)_2$ (20 mol%) and AcOH (20 mol%) in toluene at 130 °C for 15 h under air (Table 1, entry 11), and 74% isolated yield of **3a** along with 4% NMR yield of **1aa** and 9% NMR yield of **2aa** could be obtained under the optimal conditions.[11] Notably, when the ratio of **2a**/**1a** was decreased to 1.2 and the reaction time was increased to 20 h (Table 1, entry 15), the isolated yield of **3a** was slightly reduced from 74% to 66% along with a subtle change of homo-couplings. Furthermore, a moderate isolated yield of **3a** (56%) could be obtained even when the ratio of **2a**/**1a** was further decreased to 1.0 (Table 1, entry 16).

Substrate Scope. With the optimized conditions in hand, we first investigated the scope of phenols using *N*-(*tert*-butyl)benzamide (**2a)** as the model coupling partner (Scheme 4). It was found that a series of phenol substrates with either *ortho*-, *meta*-, or *para*-substituents, regardless of their electronic nature, were compatible with this catalytic system to deliver the cross-coupled products in moderate to good yields. Although both of mono- and diarylated products were observed in the case of some unsubstituted or *para*-substituted substrates, the mono-/di-selectivity could be controlled by slightly

changing the reaction conditions (**3b**, **3b'**, **3d** and **3l**). When the loading of the catalyst was reduced to 3 mol%, the monoarylation product **(3b)** was obtained as the major product in 64% yield. However, when $Cu(OAc)_2$ (5 mol%) and amide **2a** (3.0 equiv) were used, the diarylated product (**3b'**) was afforded as the predominant product in 53% yield together with 38% of **3b**. The steric hindrance at the *ortho*-position had no significant influence on the reactivity even

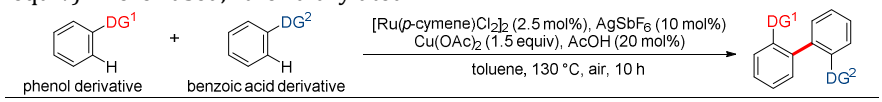

Directing Groups (DGs)	DG2a	DG2b	DG2c	DG2d	DG2e	DG2f	DG2g	DG2h	DG2i	DG2j
DG1a	n.d	n.d	n.d	trace	trace	13%[a]	trace	trace	n.d	n.d
DG1b	n.d	n.d	n.d	n.d	n.d	n.d	n.d	n.d	n.d	n.d
DG1c	n.d	n.d	n.d	n.d	trace	trace	n.d	n.d	n.d	n.d
DG1d	n.d	n.d	n.d	n.d	trace	10%[a]	trace	trace	n.d	n.d
DG1e	n.d	n.d	n.d	n.d	n.d	n.d	n.d	n.d	n.d	n.d
DG1f	n.d	n.d	n.d	n.d	n.d	n.d	n.d	n.d	n.d	n.d
DG1g	n.d	n.d	n.d	n.d	n.d	n.d	n.d	n.d	n.d	n.d
DG1h	n.d	n.d	n.d	n.d	n.d	n.d	n.d	n.d	n.d	n.d

Scheme 3. Reaction discovery and screening of directing groups. Reaction conditions: phenol derivative (0.20 mmol), benzoic acid derivative (0.40 mmol), $[Ru(p\text{-cymene})Cl_2]_2$ (2.5 mol%), $AgSbF_6$ (10 mol%), $Cu(OAc)_2$ (1.5 equiv) and AcOH (20 mol%) in toluene (0.5 mL) at 130 °C for 10 h under an air atmosphere. Determined by GC-MS analysis. [a]Yield determined by ^1H NMR analysis using CH_2Br_2 as the internal standard. n.d = not detected.

Table 1. Catalytic System Evaluation[a]

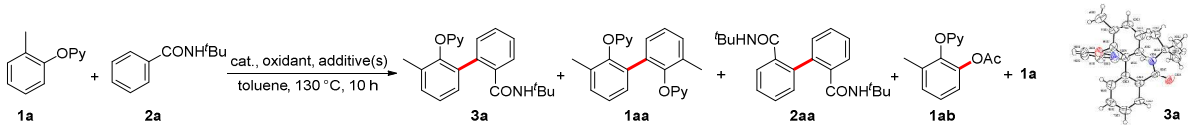

Entry	Catalyst (mol%)	Oxidant (mol%)	Additive(s)	2a/1a	Yield (%)[b]				
					3a	1aa	2aa	1ab	1a
1	$[Ru(p\text{-cymene})Cl_2]_2$ (2.5) + $AgSbF_6$ (10)	$Cu(OAc)_2$ (150) + air	AcOH	2.0	11	0	1	18	62
2	$[Ru(p\text{-cymene})Cl_2]_2$ (2.5) + $AgSbF_6$ (10)	air	AcOH	2.0	16	3	1	4	74
3	$[Ru(p\text{-cymene})Cl_2]_2$ (2.5) + $AgSbF_6$ (10)	O_2	AcOH	2.0	12	5	1	10	71
4	$[Ru(p\text{-cymene})Cl_2]_2$ (2.5) + $AgSbF_6$ (10)	$Cu(OAc)_2$ (5) + air	AcOH	2.0	36	4	5	21	41
5	$[Ru(p\text{-cymene})Cl_2]_2$ (2.5) + $AgSbF_6$ (10)	$Cu(OAc)_2$ (3) + air	AcOH	2.0	39	9	3	11	45
6	$[Ru(p\text{-cymene})Cl_2]_2$ (2.5)	$Cu(OAc)_2$ (3) + air	AcOH	2.0	0	13	0	9	77
7	$[Ru(p\text{-cymene})(MeCN)_3](SbF_6)_2$ (5)	$Cu(OAc)_2$ (3) + air	AcOH	2.0	40	14	4	9	36
8[c]	$[Ru(p\text{-cymene})(MeCN)_3](SbF_6)_2$ (5)	$Cu(OAc)_2$ (3) + air	AcOH	2.0	17	10	1	11	65
9[d]	$[Ru(p\text{-cymene})(MeCN)_3](SbF_6)_2$ (5)	$Cu(OAc)_2$ (3) + air	AcOH	2.0	45	17	5	13	18
10[d]	$[Ru(p\text{-cymene})(MeCN)_3](SbF_6)_2$ (5)	$Cu(OAc)_2$ (3) + air	AcOH/$Zn(OTf)_2$	2.0	68	4	7	9	17
11[d,e]	$[Ru(p\text{-cymene})(MeCN)_3](SbF_6)_2$ (5)	$Cu(OAc)_2$ (3) + air	AcOH/$Zn(OTf)_2$	2.0	80(74)	4	9	8	6
12[d,f]	$[Ru(p\text{-cymene})(MeCN)_3](SbF_6)_2$ (5)	$Cu(OAc)_2$ (3) + air	AcOH/$Zn(OTf)_2$	2.0	76	5	11	8	4
13[d,e]	$[Ru(p\text{-cymene})(MeCN)_3](SbF_6)_2$ (5)	$Cu(OAc)_2$ (3) + air	AcOH/$Zn(OTf)_2$	1.5	67	6	7	9	13
14[d,f]	$[Ru(p\text{-cymene})(MeCN)_3](SbF_6)_2$ (5)	$Cu(OAc)_2$ (3) + air	AcOH/$Zn(OTf)_2$	1.5	74	6	9	10	7
15[d,f]	$[Ru(p\text{-cymene})(MeCN)_3](SbF_6)_2$ (5)	$Cu(OAc)_2$ (3) + air	AcOH/$Zn(OTf)_2$	1.2	71(66)	7	7	12	8
16[d,f]	$[Ru(p\text{-cymene})(MeCN)_3](SbF_6)_2$ (5)	$Cu(OAc)_2$ (3) + air	AcOH/$Zn(OTf)_2$	1.0	64(56)	9	5	14	10

[a]Reaction conditions: **1a** (0.20 mmol), **2a**, catalyst, oxidant and additive(s) (20 mol%) in toluene (0.5 mL) at 130 °C for 10 h under the indicated atmosphere. [b]NMR yields are based on **1a (**for **3a**, **1aa**, **1ab** and **1a)** or **2a** (for **2aa**) using CH_2Br_2 as the internal standard. Isolated yield is in parenthesis. [c]Toluene (1.0 mL) was used. [d]Toluene (0.3 mL) was used. [e]Run for 15 h. [f]Run for 20 h.

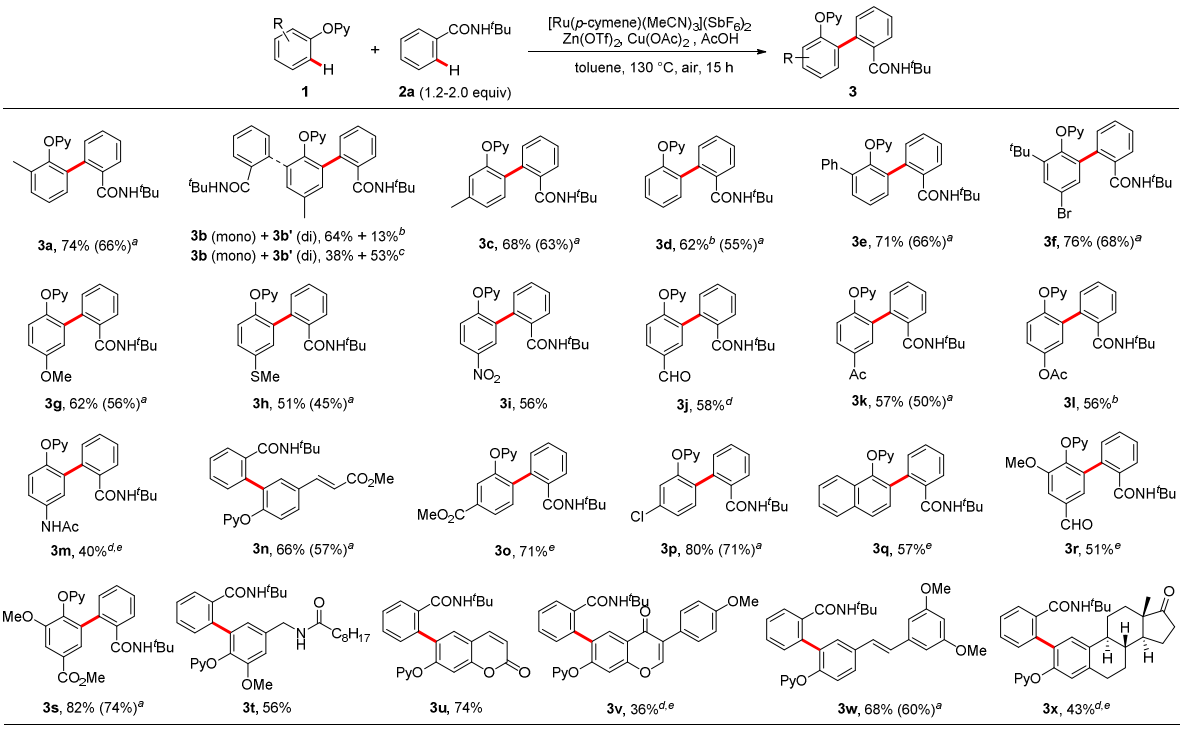

Scheme 4. Scope of phenols. Reaction conditions: **1** (0.20 mmol), **2a** (0.40 mmol), [Ru(*p*-cymene)(MeCN)$_3$](SbF$_6$)$_2$ (5 mol%), Cu(OAc)$_2$ (3 mol%), Zn(OTf)$_2$ (20 mol%) and AcOH (20 mol%) in toluene (0.3 mL) at 130 °C for 15 h under air. Isolated yield. [a]1.2 equiv of **2a** was used and run for 20 h. [b][Ru(*p*-cymene)(MeCN)$_3$](SbF$_6$)$_2$ (3 mol%) was used. [c]3.0 equiv of **2a** and 5 mol% of Cu(OAc)$_2$ were used. [d]Run for 20 h. [e]Run at 140 °C.

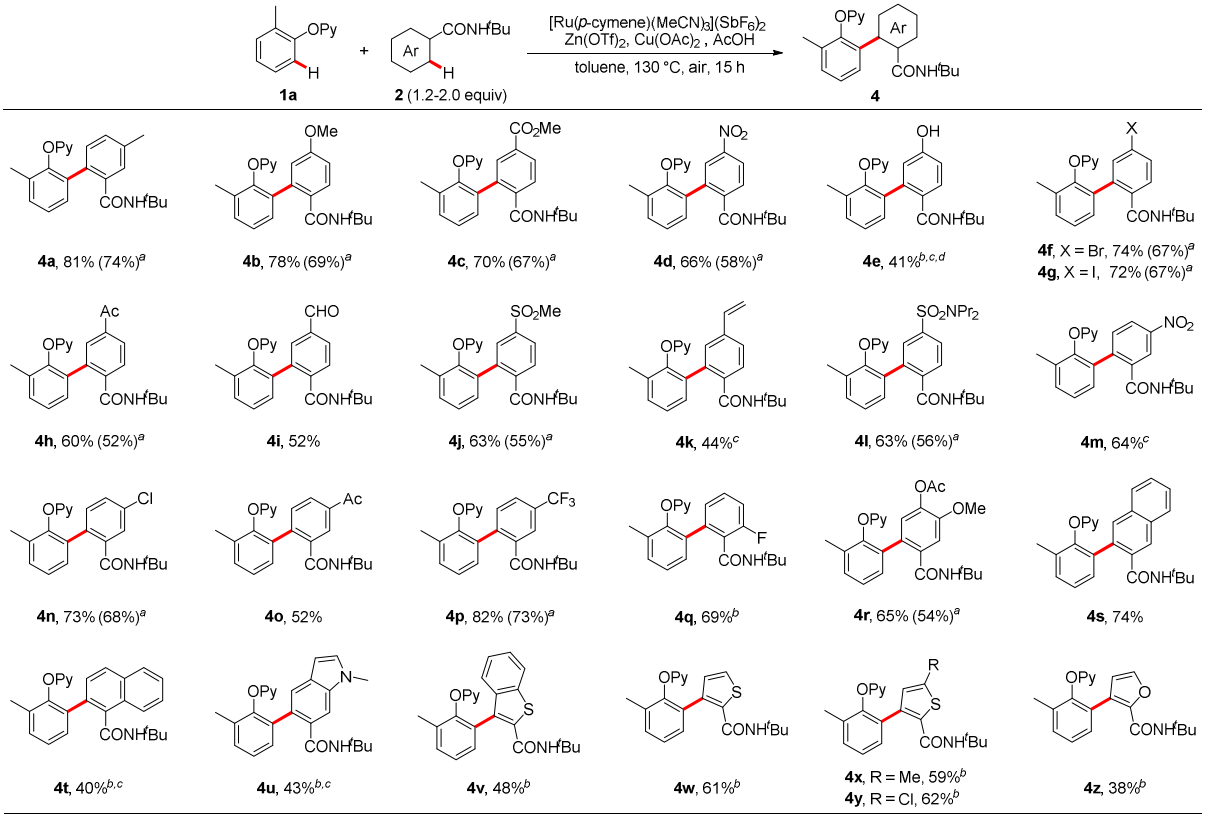

Scheme 5. Scope of (hetero)aromatic amides. Reaction conditions: **1a** (0.20 mmol), **2** (0.40 mmol), [Ru(*p*-cymene)(MeCN)$_3$](SbF$_6$)$_2$ (5 mol%), Cu(OAc)$_2$ (3 mol%), Zn(OTf)$_2$ (20 mol%) and AcOH (20 mol%) in toluene (0.3 mL) at 130 °C for 15 h under air. Isolated yield. [a]1.2 equiv of **2** was used and run for 20 h. [b]Run at 140 °C. [c]Run for 20 h. [d]Cu(OAc)$_2$ (5 mol%) was used.

when a bulky *tert*-butyl group is incorporated (**3f**). A broad scope of reactive groups such as bromide (**3f)**, methoxy (**3g**), methylthio (**3h**), nitro (**3i**), formyl (**3j**), acetyl (**3k**), acetoxyl (**3l**), acylamino (**3m**), alkenyl (**3n**), ester (**3o**), and chloride (**3p**) were all tolerated in this reaction. To our delight, this method was tolerant of more complex natural product derivatives, such as vanillin (**3r**), vanillic acid (**3s**), nonivamide (**3t**), 7-hydroxycoumarin (**3u**), formononetin (**3v**), pterostilbene (**3w**) and estrone (**3x**), thus providing an opportunity for late-stage functionalization. Remarkably, even only 1.2 equiv of **2a** was used to react with selected phenols, the cross-coupled products could also be obtained in moderate to good yields (**3a, 3c-3h, 3k, 3n, 3p, 3s** and **3w**).

Subsequently, we evaluated the scope of (hetero)aromatic amides (Scheme 5). The amides bearing both electron-donating and electron-withdrawing groups were suitable coupling partners. A variety of sensitive functional groups, including methoxy (**4b**), ester (**4c**), nitro (**4d** and **4m**), hydroxyl (**4e**), bromide (**4f**), iodide (**4g**), acetyl (**4h** and **4o**), formyl (**4i**), sulfone (**4j**), vinyl (**4k**), sulfamoyl (**4l**), chloride (**4n**), and fluorine (**4q**) were tolerated well. The reaction with *meta*-substituted *N*-(*tert*-butyl)benzamide exclusively occurred at the less congested *ortho* site (**4a, 4m-4p**). In the case of *N*-(*tert*-butyl)-2-naphthamide, the coupling reaction regioselectively took place at the less crowded 3-position in 74% yield (**4s**). A diminished yield was attained when *N*-(*tert*-butyl)-1-naphthamide was attempted (**4t**). Moreover, heteroarenes such as indole (**4u**), benzothiophene (**4v**), thiophenes (**4w-y**) and furan (**4z**) were also effective substrates. It is notable that 1.2 equiv of amides could also deliver the corresponding products in moderate to high yields (**4a-4d, 4f-4h, 4j, 4l, 4n, 4p** and **4r**).

To further demonstrate the synthetic utility of this protocol, a gram-scale reaction and the removal of the directing groups were conducted (Scheme 6). A 61% yield of **3a** was given when the reaction was performed on a 5 mole scale. Remarkably, only 0.5 mL of toluene (about 1.0 equiv) was used as the solvent. To our delight, both directing groups were removed under the condition for the removal of pyridyl, giving the *6H*-benzo[*c*]chromen-6-one derivative (**5**) after acidification. Further treatment with methyl iodide, the methyl group protected 2'-hydroxybiphenyl-2-carboxylic acid derivative (**6**) was obtained in 83% overall yield.

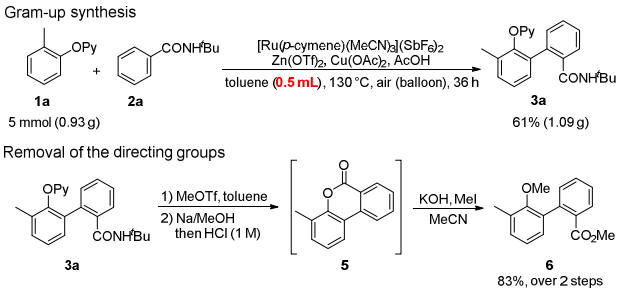

Scheme 6. Gram-up synthesis and removal of the directing groups

Synthetic Application. Palomid 529 (also called RES-529), an inhibitor of PI3K/Akt/mTOR, is currently being developed in oncology and ophthalmology.[6e,12] In 2015, the orphan drug designation for Palomid 529 to treat glioblastoma multiforme was granted by the US Food and Drug Administration (FDA). Besides, two Phase I clinical trials of Palomid 529 in the treatment of neovascular age-related macular degeneration has been completed. In the existing synthetic route, Palomid 529 is synthesized in ten steps starting from 5-bromoisovanillin and the construction of the biaryl scaffold is completed through Suzuki coupling reaction (Scheme 7a).[13] To further elucidate the applicability of our methodology, a concise synthesis of Palomid 529 was performed in only 7 steps starting from 4-methoxyphenol (Scheme 7b). First, the reaction of 4-methoxyphenol with 2-bromopyridine afforded 2-(4-methoxyphenoxy)pyridine **1g** in 88% yield. Then, the iodination at the *ortho*-position of the methoxyl group using *N*-iodosuccinimide gave **7** in 77% yield. Subsequently, the Ru(II)-catalyzed oxidative C–H/C–H cross-coupling reaction of **7** with 3-acetyl-*N*-(*tert*-butyl)benzamide **2p** furnished the biaryl **8** in 61% yield. The biaryl was next subjected to Cu-catalyzed Ullmann

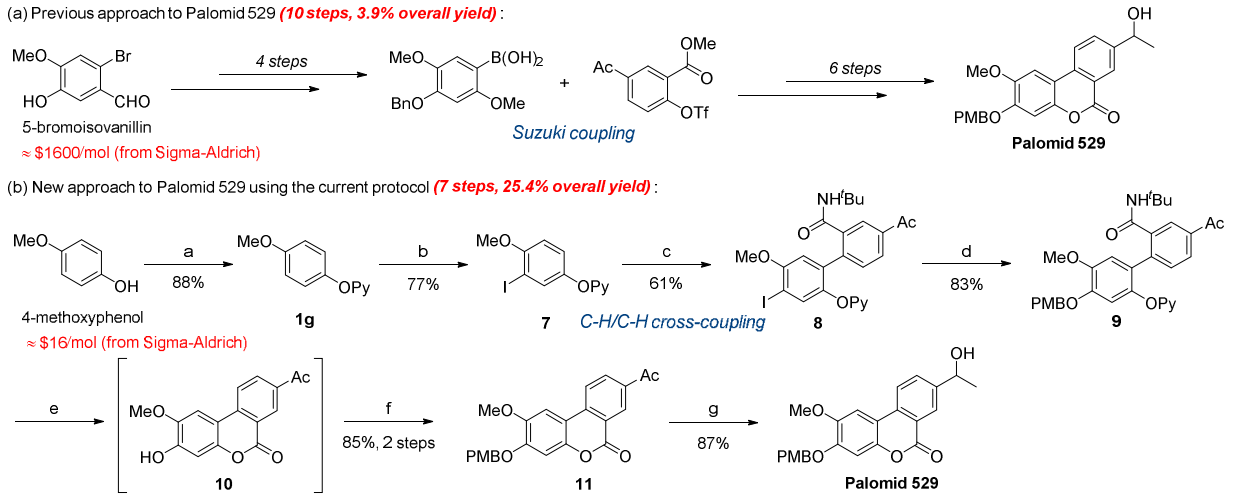

Scheme 7. Synthesis of Palomid 529. Reaction conditions: (a) 2-bromopyridine, CuI, 2-picolinic acid, K_3PO_4, DMSO, 90 °C, 24 h; (b) NIS, TsOH·H_2O, MeCN, 60 °C, 10 h; (c) 3-acetyl-*N*-(*tert*-butyl)benzamide (**2p**), [Ru(*p*-cymene)(MeCN)$_3$](SbF$_6$)$_2$, Cu(OAc)$_2$, Zn(OTf)$_2$, AcOH, toluene, 130 °C, 15 h; (d) PMB-OH, CuI, Me_4Phen, Cs_2CO_3, toluene, 110 °C, 24 h; (e) MeOTf, toluene, 100 °C, 2 h, then Na/MeOH, 80 °C, 0.5 h, next HCl (1 M), rt, 0.5 h; (f) PMB-Br, K_2CO_3, DMF, 80 °C, 12 h; (g) $NaBH_4$, DCM/MeOH, rt, 3 h. NIS = *N*-iodosuccinimide, PMB-OH = 4-methoxybenzyl alcohol, Me_4Phen = 3,4,7,8-tetramethylphenanthroline, PMB-Br = 4-methoxybenzyl bromide.

reaction with 4-methoxybenzyl alcohol to yield the etherified product **9** in 83% yield. Notably, when the iodine group of **8** was replaced by the bromine group, a low conversion (about 20%) was observed even under harsher reaction conditions, which clearly demonstrates an importance of excellent functionality compatibility of the established methodology. The removal of directing groups led to a lactone product **10** along with an elimination of the 4-methoxylbenzyl moiety. Thus, the resulting product was next treated with 4-methoxybenzyl bromide. Finally, the reduction of the acetyl group of **11** using sodium borohydride gave rise to Palomid 529 in 87% yield. Compared with the previous procedure, we herein presented a more concise (7 steps *vs.* 10 steps) and efficient synthetic route (25.4% overall yield *vs.* 3.9% overall yield) to Palomid 529 starting from a much cheaper commodity chemical ($16/mol for 4-methoxyphenol *vs.* $1600/mol for 5-bromoisovanillin).

Mechanistic Experimental Study. To gain a more detailed mechanistic insight of this reaction, a series of experiments were performed. Firstly, the deuterium-labeling experiments were conducted (Scheme 8). Treatment of **1a** with D_2O under the standard conditions could lead to a significant deuterium incorporation both in the presence and absence of **2a**, indicating that the C–H activation process of the phenol substrate is reversible (Scheme 8a and 8c). However, only a small amount of deuterated **2a** was obtained in the absence of **1a** (7% D, Scheme 8b) and an obvious H/D scrambling was observed for **2a** in the presence of **1a** (35% D, Scheme 8c). In addition, a similar H/D exchange of compound **2a** was observed (37% D) when the non-productive phenol substrate **1y** was used instead of **1a** (Scheme 8d). These results suggest that the enhanced H/D exchange of **2a** could be attributed to the coordination effect of the pyridyl group to the ruthenium catalyst, which might stabilize the ruthenacyclic intermediate of amide.

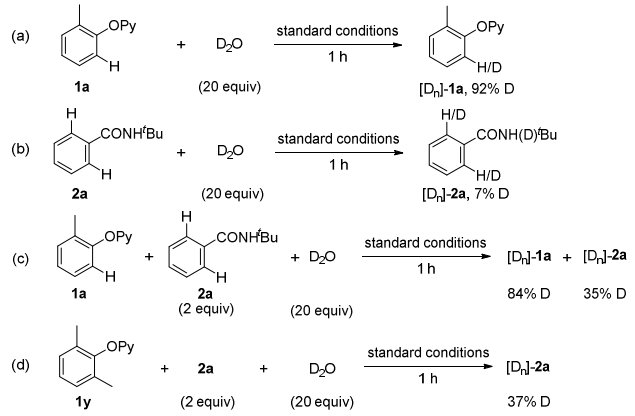

Scheme 8. Deuterium labeling experiments

Subsequently, kinetic isotope effect (KIE) experiments for both coupling partners were carried out (Scheme 9). A significant kinetic isotope effect (k_H/k_D = 2.5) was observed for the parallel reactions between **1a** or [D_1]-**1a** with **2a**. However, a low KIE value of 1.1 was determined for amide. These findings suggest that the C–H cleavage of **1a** might be involved in the rate-limiting step and the cyclometalation of **2a** was not involved in the rate-limiting step.

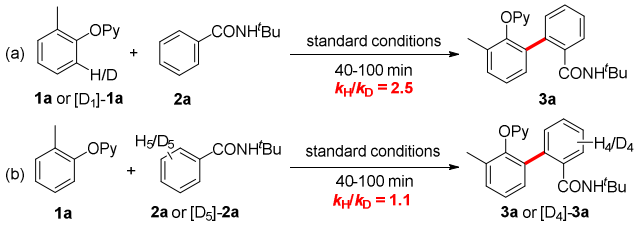

Scheme 9. Kinetic isotope effect (KIE) studies

The control experiments were implemented with stoichiometric amounts of [Ru(*p*-cymene)Cl_2]$_2$ (Scheme 10).[14] Treatment of **1a** with **2a** under air smoothly afforded the desired cross-coupled product **3a** in 36% isolated yield. However, only a trace amount of **3a** was detected when the

reaction was conducted under an inert atmosphere. The contrasting results illustrate that a Ru(II)/Ru(0) catalytic cycle might be ruled out in the process.

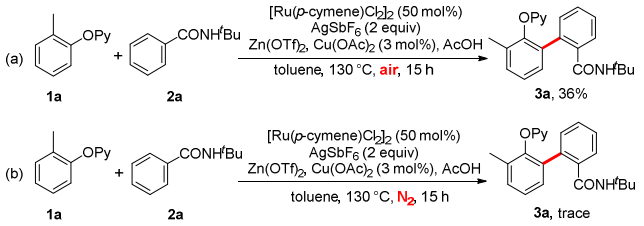

Scheme 10. Control experiments

Two cyclometalated Ru(II) complexes were synthesized. The neutral six-membered ruthenacyclic complex **I** was prepared via the reaction of 2-(*p*-tolyloxy)pyridine (**1b**) with $[Ru(p\text{-cymene})Cl_2]_2$ in the presence of $AgSbF_6$ (Scheme 11a). It is worthy of note that only a trace amount of **I** was detected in absence of $AgSbF_6$. However, the preparation of ruthenacyclic complex of amide failed when treatment of **2a** under otherwise identical conditions. Fortunately, the pyridyl-coordinated cationic five-membered ruthenacycle **II** of amide was generated when **1b** reacted with **2a** at a molar ratio of 1:2, and no ruthenacycle of **1b** was detected (Scheme 11b). This result implies that the pyridyl group enables to stabilize the forming ruthenacyclic complex of amide by the coordination to the ruthenium center. Both of the ruthenacyclic complexes were isolated and fully confirmed by NMR spectroscopy and X-ray crystallography (Figure 1). Then the reactivities of **I** and **II** were examined. When they were designated as the catalyst (3 mol%) for the cross-coupling reaction of **1b** with **2a**, the comparable activities was observed and the reaction yields were similar to those under the standard conditions (Scheme 11c and 11d). When a stoichiometric amount of complex **I** or **II** reacted with **2a**, similar results were obtained (Scheme 11e and 11f). Furthermore, treatment of complex **I** with 2.0 equivalent of **2a** in the presence of either KOAc or AcOH and $AgSbF_6$ delivered complex **II** in 22% and 9% isolated yields, respectively (Scheme 11g and 11h). These transformations indicate that the cationic ruthenacyclic complexes of amides are more thermodynamically stable than their 2-aryloxypyridines analogues. Based on these results, we speculate that the complex **II** could be a reaction intermediate in this transformation and the first C–H bond activation could preferentially take place at the amide in the cross-coupling pathway.

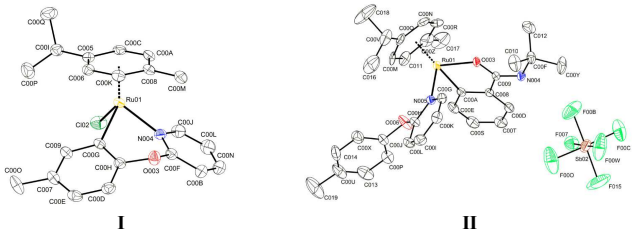

Figure 1. ORTEP diagrams of complexes **I** and **II**. Thermal ellipsoids are shown at the 30% probability level. Hydrogen atoms are omitted for clarity.

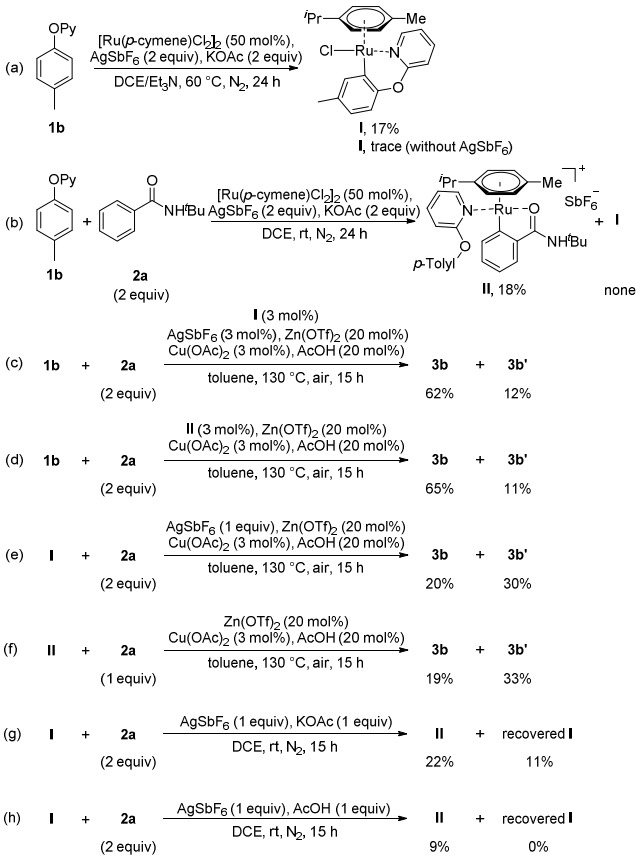

Scheme 11. Synthesis, activity and transformations of ruthenacycle complexes

Mechanistic Computational Study. Density functional theory (DFT) calculation was employed to clarify detailed mechanism and the chemoselectivity for the Ru(II)-catalyzed oxidative C–H/C–H cross-coupling reaction. In the theoretical calculation, density functional M11-L[15] proposed by Truhlar group was employed to calculate free energies in toluene based on B3LYP[16] optimized stationary points on potential energy profiles.[17] As depicted in Figure 2, two competitive pathways were considered in the theoretical study and the cationic ruthenium complex **12** plus all of the reaction components was chosen as the relative zero for the free energy profiles. In pathway A (blue lines), the first C–H cleavage takes place with the carbamoyl substituted reactant **2a** followed by the second C–H cleavage with the 2-pyridinyloxy substituted reactant **1d**. The coordination of reactant **2a** to the ruthenium center affords carbamoyl chelate Ru(II) complex **13**, with free energy decrease of 7.4 kcal/mol. The first concerted metalation-deprotonation (CMD) process occurs via transition state **14-ts**, leading to the generation of aryl–Ru(II) intermediate **15**, with an activation free energy of 20.5 kcal/mol. The pyridine coordinated aryl–Ru(II) intermediate **16** could then be generated after ligand exchange between the reactant **1d** and AcOH. The relative free energy of **16** is 6.2 kcal/mol lower than that of **15**, which is in consistence with the deuterium labeling experiments shown in Scheme 8. In the presence of $Cu(OAc)_2$, two-step single electron oxidation to yield a hepta-coordinated Ru(IV) complex **19** are endergonic by 7.1 kcal/mol. Subsequently, the second C–H bond cleavage proceeds via another CMD type of transition state **20-ts**,

which forms a diaryl–Ru(IV) intermediate **21**, with a free energy barrier of 20.9 kcal/mol.

Alternatively, the order of C–H cleavage with the carbamoyl substituted reactant **2a** and the pyridinyloxy substituted reactant **1d** was changed in pathway B. As the description of red lines in Figure 2, the diaryl–Ru(IV) intermediate **21** could also be generated through another competitive pathway. The coordination of 2-phenoxypyridine **1d** to the ruthenium center affords the pyridine chelate Ru(II) complex **23**. The relative free energy of complex **23** is 3.7 kcal/mol lower than that of intermediate **13**, which indicates that the pyridine directing group exhibits enhanced coordinating ability. The first C–H bond cleavage of 2-phenoxypyridine in Ru(II) complex **23** takes place via transition state **24-ts**, generating aryl–Ru(II) intermediate **25** reversibly. The activation free energy for this process has been determined to be 22.0 kcal/mol. The activation barrier in this step is 1.5 kcal/mol higher than the corresponding step of carbamoyl directed C–H cleavage in pathway A. However, the relative free energy of transition state **24-ts** is 2.2 kcal/mol lower than that of **14-ts**. The lower relative free energy of **24-ts** could be attributed to the enhanced coordinating ability of the pyridine directing group. Subsequent ligands exchange affords amide coordinated aryl–Ru(II) intermediate **26**, from which the hepta-coordinated Ru(IV) complex **27** is generated endothermically after oxidation by $Cu(OAc)_2$. The second C–H bond activation step then proceeds via transition state **28-ts**, forming the same diaryl–Ru(IV) intermediate **21**, with a free energy barrier of 26.6 kcal/mol. The relative free energy of transition state **28-ts** is 10.5 kcal/mol higher than that of **20-ts**, which is contributed in part by thermodynamic instability of metallacycle intermediate **27**. Therefore, calculated results suggest that reaction pathway A via the first C–H bond cleavage of amide reactant, oxidation by $Cu(OAc)_2$, and second C–H bond cleavage of phenoxypyridine reactant was more favorable. With the diaryl–Ru(IV) intermediate **21** in hand, the following reductive elimination proceeds rapidly via transition state **22-ts** with a free energy barrier of only 0.1 kcal/mol. The cross-coupled product **3d** was then released irreversibly, and the Ru(II) active catalyst **23** was also regenerated concurrently. Throughout the catalytic cycle, the overall activation free energy for the energy profile was determined to be 30 kcal/mol (**20-ts**), indicating that this reaction could proceed smoothly under this reaction condition. In the theoretical calculations, the second C–H bond cleavage of 2-phenoxypyridine was considered as a rate-limiting step for the catalytic cycle, which is consistent with kinetic isotope effect observations.

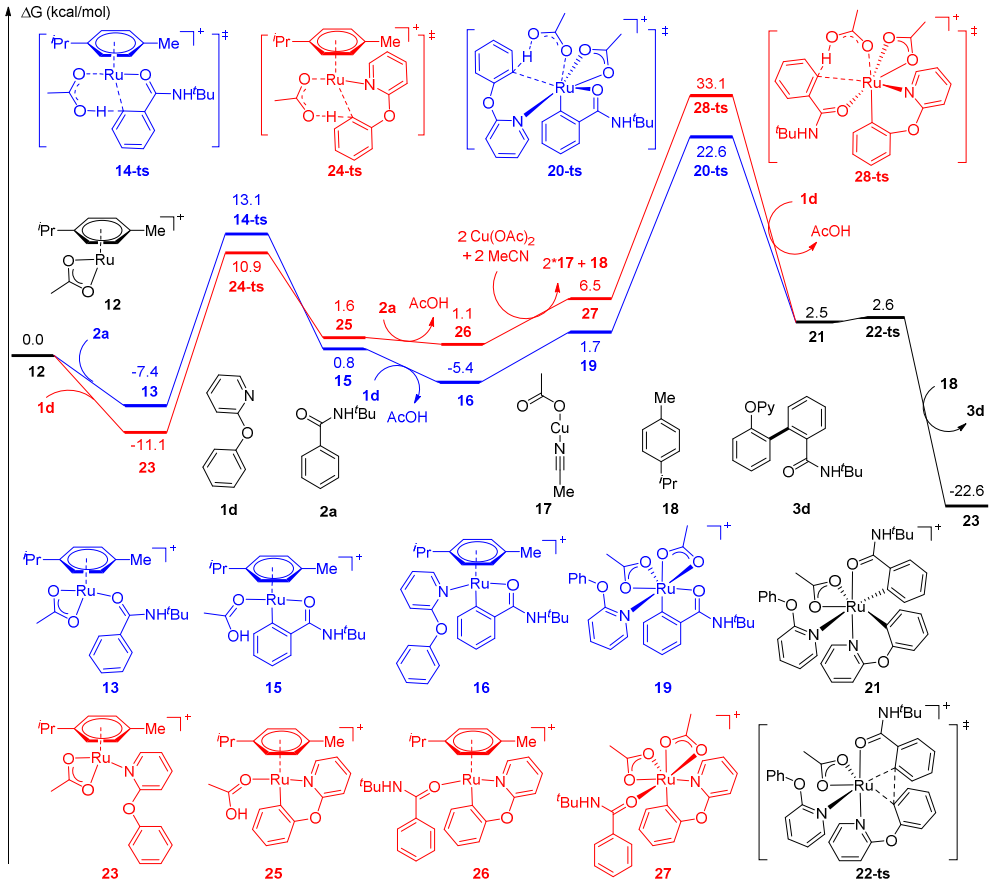

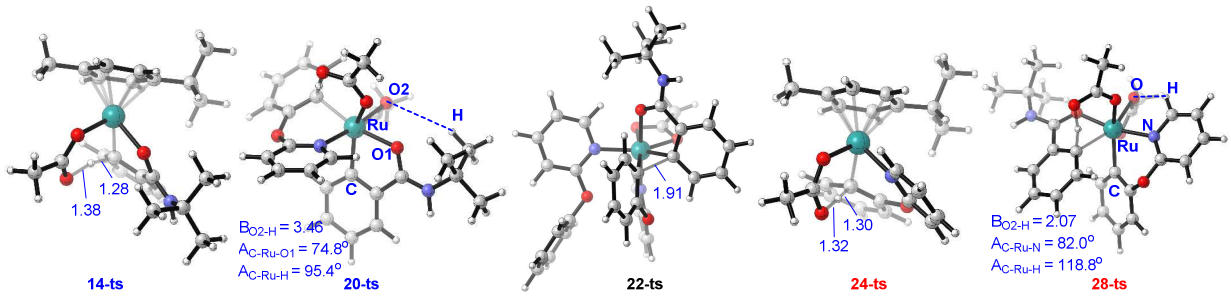

Figure 2. Free energy profiles of two competitive pathways (pathway A (blue line) and pathway B (red line)) for the generation of oxidative C–H/C–H cross-coupling product. The values have been given in the unit of kcal/mol and represent the relative free energies calculated using the M11-L method in toluene solvent. The bond lengths are given in angstroms.

We also considered the side pathways for the generation of acyloxylated or homo-coupled products of 2-phenoxypyridine. The calculated results are summarized in Figure 3. Starting from the common hepta-coordinated 18-electron Ru(IV) intermediate **27**, the dissociation of **2a** affords a hexa-coordinated 16-electron intermediate **29** with free energy increase of 7.2 kcal/mol. The subsequent C–O bond reductive elimination via transition state **30-ts** leads to the formation of acyloxylated product **31** and regenerates Ru(II) catalyst **12**. The relative free energy of transition state **30-ts** is 3.1 kcal/mol higher than that of **20-ts**, indicating that the acyloxylated product **31** would be observed as a side product under the current reaction conditions. We also considered a C–O bond reductive elimination from a hepta-coordinated 18-electron Ru(IV) intermediate **32**. However, the relative free energy of **37-ts** is much higher than that of **30-ts**. Meanwhile, the pyridine coordinated intermediate **32** could be generated after the ligands exchange, from which the second C–H bond cleavage occurs through transition state **33-ts** with a free energy barrier of 22.7 kcal/mol to generate diaryl–Ru(IV) intermediate **34**. The following C–C bond reductive elimination then proceeds rapidly via transition state **35-ts** with release of phenoxypyridine homo-coupled product **36**. The relative free energy of transition state **33-ts** is 4.8 kcal/mol higher than that of **20-ts**, which suggests that the homo-coupling is kinetically unfavorable, in agreement with the experimental result.[18] Further structure analysis showed that in transition state **33-ts** the bond angle $A_{C\text{-}Ru\text{-}N}$ was 82.2°, and the flare angle $A_{C\text{-}Ru\text{-}H}$ was up to 119.8°, while the corresponding flare angles $A_{C\text{-}Ru\text{-}O1}$ and $A_{C\text{-}Ru\text{-}H}$ in **20-ts** were determined to be 74.8° and 95.4°, respectively. The wider flare angles indicate that the 2-pyridyloxy directing group performs larger steric hindrance, which results in the high activation free energy of transition state **33-ts**.

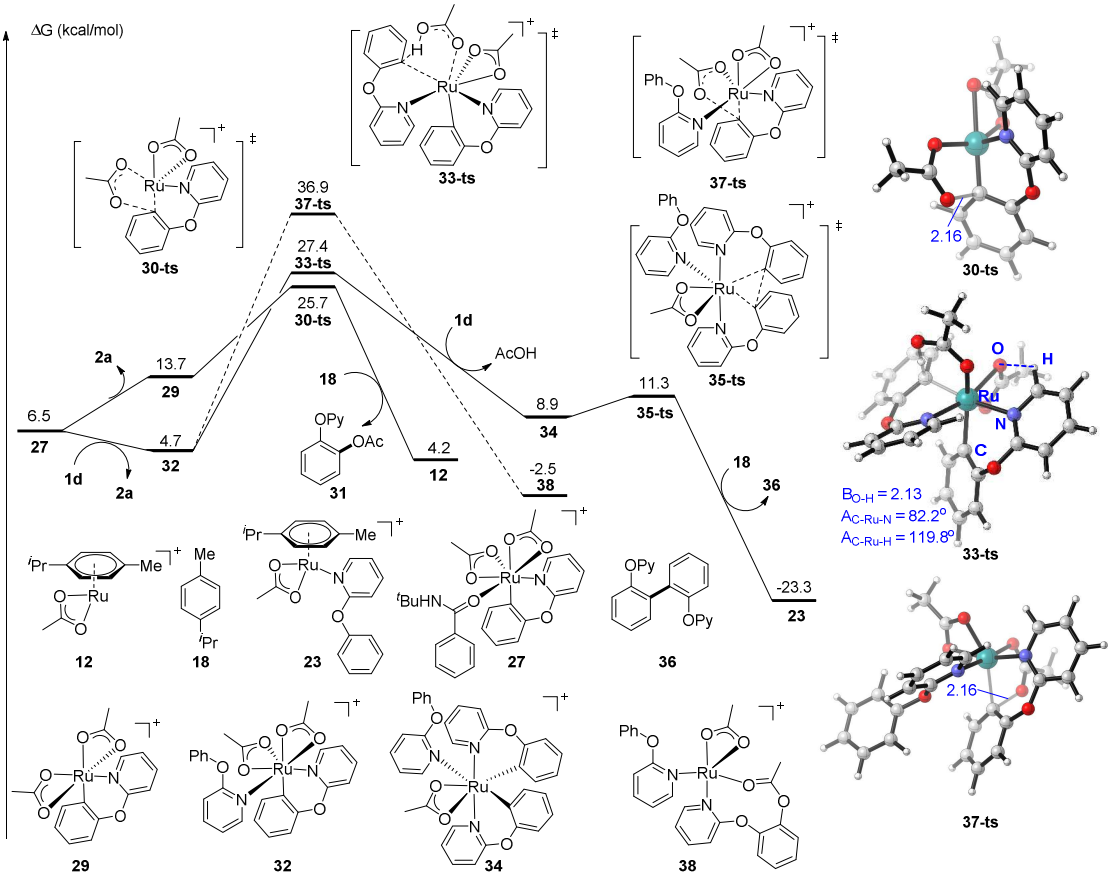

Figure 3. Free energy profiles for the generation of side products. The values have been given in the unit of kcal/mol and represent the relative free energies calculated using the M11-L method in toluene solvent. The bond lengths are given in angstroms.

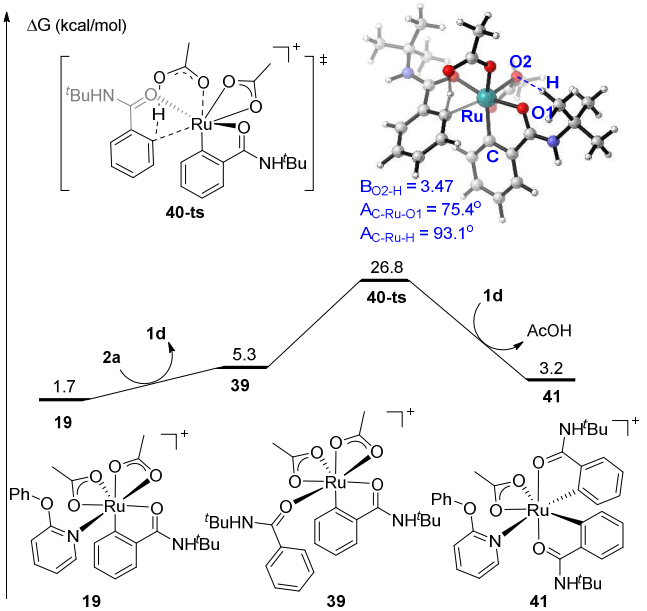

Figure 4. Free energy profiles for the generation of homo-coupled product for reactant **2a**. The values have been given in the unit of kcal/mol and represent the relative free energies calculated using the M11-L method in toluene solvent. The bond lengths are given in angstroms.

In addition, the side pathway to generate amide homo-coupled product has also been considered. As shown in Figure 4, the ligand exchange between intermediate **19** and reactant **2a** affords intermediate **39**, with a free energy increase of 3.6 kcal/mol. This energy discrepancy suggests that the amide group exhibits subdued coordinating ability. Subsequent C–H bond cleavage leads to the generation of diaryl–Ru complex **41**. Although the steric hindrance is avoided in transition state **40-ts**, the relative free energy of transition state **40-ts** is 4.2 kcal/mol higher than that of **20-ts** in cross-coupling pathway. This high relative free energy of **40-ts** would be partly contributed to the weakly coordinating ability of reactant **2a**. It indicates that the homo-coupling process of **2a** is also unfavorable compared with the cross-coupling, in accordance with the experimental result.[19]

On the basis of the above investigations, we could reach a following conclusion by DFT calculation. Although amide **2a** is less kinetically favorable than 2-phenoxypyridine **1d** in the first CMD process, the resulting ruthenium cycle of amide **2a** is more competitive in the C–H metalation of the second coupling partner owing to its less steric hindrance. Meanwhile, the relatively large steric hindrance of 2-pyridyloxyl group can subdue the tendency of homo-coupling of **1d** under the present Ru catalytic system. On the other hand, the relatively strong coordinating ability of 2-pyridyloxy group not only renders **1d** more easily to bind to ruthenium central and further stabilize the ruthenacyclic intermediate of amide **2a** formed in the first C–H metalation process, but also facilitates the second C–H activation at 2-phenoxypyridine **1d**, thus leading to the cross-coupling other than homo-coupling of amide **2a**.

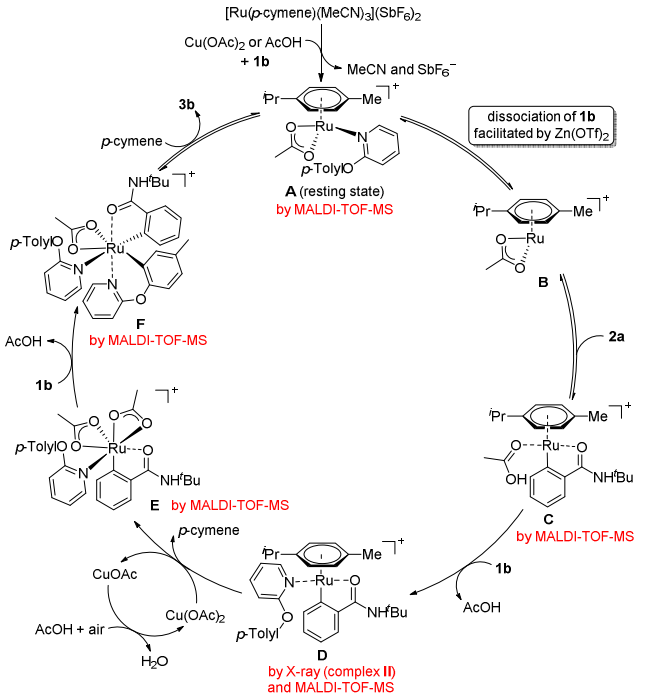

Scheme 12. Plausible catalytic cycle

Mechanistic Proposal. On the basis of the above experimental and theoretical studies, a plausible catalytic cycle is proposed (Scheme 12). Initially, the cationic Ru(II) species **A**, detected by MALDI-TOF-MS (calcd: 480.11, found: 480.13), is generated from $[Ru(p\text{-cymene})(MeCN)_3](SbF_6)_2$ in the presence of substrate **1b** and acetic acid or acetate. Because the strongly coordinated **1b** inhibits the binding of amide **2a** to the ruthenium center, it is required to generate the coordinatively unsaturated Ru(II) species **B** by releasing **1b** from the resting state species **A**.[20] We propose that the addition of $Zn(OTf)_2$ could help dissociation of the coordinated **1b** from **A** through the coordination of 2-pyridinyl to $Zn(OTf)_2$. Next, **2a** coordinates to **B** and undergoes a reversible C–H bond activation to give ruthenacycle **C**, detected by MALDI-TOF-MS ([M-AcOH] calcd: 412.12, found: 412.12). Ligand exchange of the coordinated AcOH with substrate **1b** leads to a more thermodynamically stable complex **D**, characterized by X-ray (complex **II**) and detected by MALDI-TOF-MS (calcd: 597.21, found: 597.27). In the presence of $Cu(OAc)_2$ and air, the Ru(II) complex **D** is oxidized to the Ru(IV) species **E**,[3b,21] detected by MALDI-TOF-MS (calcd: 581.12, found: 581.16). Although air alone could act as an oxidant to promote this reaction, the reaction efficiency is very low (Table 1, entry 2). Thus, we propose that air mainly acts as the terminal oxidant to oxidize the Cu salt in this reaction. Thereafter, the bis-cyclometalated Ru(IV) intermediate **F**, detected by MALDI-TOF-MS (calcd: 706.19, found: 706.16), is produced through the second cyclometalation process, which is considered as the rate-limiting step in the catalytic cycle (supported by the kinetic isotope effect study and DFT calculation). Then, reductive elimination of the high-valent diarylruthenium complex **F** gives the cross-coupled product **3b**, detected by MALDI-TOF-MS ($[M+H]^+$ calcd: 361.19, found: 361.15). Simultaneously, the re-coordination of *p*-cymene regenerates the Ru(II) species **A** to complete the catalytic cycle. It should be noted that coordination of other ligands such as substrates, acetonitrile or solvent rather than *p*-cymene to regenerate the catalytically active Ru(II) species cannot be ruled out at the current stage.

CONCLUSIONS

In summary, we have developed an aerobic Ru(II)-catalyzed cross-coupling reaction of phenols with aromatic amides based on the dual chelation-assisted strategy. $Zn(OTf)_2$ is required to help the release of the strongly coordinating 2-aryloxypyridine **1** from the resting state species to give an active species, improving the reaction efficiency. The reaction features high chemoselectivity, complete regioselectivity, broad substrate scope, low molar ratio of substrates and excellent functionality tolerance. A concise and efficient synthetic route to Palomid 529, a new drug in development for the treatment of glioblastoma and neovascular age-related macular degeneration, has been established using the protocol developed herein as the key step. Detailed mechanistic studies are conducted by means of experimental and computational methods. A catalytic cycle involving a Ru(II)-Ru(IV)-Ru(II) process is proposed. Experimental and computational investigations indicate that the first C–H bond activation step takes place at the aromatic amide substrate and the following C–H bond activation of the 2-aryloxypyridine is involved in the rate-determined step. The origin of chemoselectivity of cross-coupling over homo-coupling is mainly ascribed to the combined effect of the relatively stronger coordinating ability of 2-aryloxypyridine and the less steric hindrance of aromatic amide. The present findings represent a pregnant guidance for the study on oxidative C–H/C–H cross-coupling between coordinating functionality-containing arenes via the dual chelation-assisted strategy.

ASSOCIATED CONTENT

Supporting Information.

Detailed information on experimental procedures, characterization data, computational calculations, crystallographic and spectroscopic data, and X-ray crystal structures (CIF) of **3a** (CCDC-1818271), **I** (CCDC-1818272), and **II** (CCDC-1818273), are available in the Supplementary Information. This material is available free of charge via the internet at http://pubs.acs.org.

AUTHOR INFORMATION

Corresponding Author

*jsyou@scu.edu.cn

*lanyu@cqu.edu.cn

Notes

The authors declare no competing financial interests.

ACKNOWLEDGMENT

The authors acknowledge the financial support from National NSF of China (Nos 21432005 and 21772020) and the Comprehensive Training Platform of Specialized Laboratory, College of Chemistry, Sichuan University.

REFERENCES

(1) For selected reviews, see: (a) Cho, S. H.; Kim, J. Y.; Kwak, J.; Chang, S. Recent Advances in the Transition Metal-Catalyzed Twofold Oxidative C–H Bond Activation Strategy for C–C and C–N Bond Formation. *Chem. Soc. Rev.* **2011**, *40*, 5068–5083. (b) Yeung, C. S.; Dong, V. M. Catalytic Dehydrogenative Cross-Coupling: Forming Carbon–Carbon Bonds by Oxidizing Two Carbon–Hydrogen Bonds. *Chem. Rev.* **2011**, *111*, 1215–1292. (c) Kuhl, N.; Hopkinson, M. N.; Wencel-Delord, J.; Glorius, F. Beyond Directing Groups: Transition-Metal-Catalyzed C–H Activation of Simple Arenes. *Angew. Chem., Int. Ed.* **2012**, *51*, 10236–10254. (d) Liu, C.; Yuan, J.; Gao, M.; Tang, S.; Li, W.; Shi, R.; Lei, A. Oxidative Coupling between Two Hydrocarbons: An Update of Recent C–H Functionalizations. *Chem. Rev*. **2015**, *115*, 12138–12204. (e) Lv, F; Yao, Z.-J. Recent Advances in Direct Dehydrogenative Biphenyl Couplings. *Sci. China Chem*. **2017**, *60*, 701–720. (f) Yang, Y.; Lan, J.; You, J. Oxidative C–H/C–H Coupling Reactions between Two (Hetero)arenes. *Chem. Rev*. **2017**, *117*, 8787–8863.

(2) For selected examples, see: (a) Zhao, X.; Yeung, C. S.; Dong, V. M. Palladium-Catalyzed *ortho*-Arylation of *O*-Phenylcarbamates with Simple Arenes and Sodium Persulfate. *J. Am. Chem. Soc.* **2010**, *132*, 5837–5844. (b) Wencel-Delord, J.; Nimphius, C.; Patureau, F. W.; Glorius, F. [$Rh^{III}Cp^*$]-Catalyzed Dehydrogenative Aryl–Aryl Bond Formation. *Angew. Chem., Int. Ed.* **2012**, *51*, 2247–2251. (c) Dong, J.; Long, Z.; Song, F.; Wu, N.; Guo, Q.; Lan, J.; You, J. Rhodium or Ruthenium-Catalyzed Oxidative C–H/C–H Cross-Coupling: Direct Access to Extended π-Conjugated Systems. *Angew. Chem. Int. Ed.* **2013**, *52*, 580–584. (d) Reddy, V. P.; Qiu, R.; Iwasaki, T.; Kambe, N. Rhodium-Catalyzed Intermolecular Oxidative Cross-Coupling of (Hetero)arenes with Chalcogenophenes. *Org. Lett.* **2013**, *15*, 1290–1293. (e) Wang, Y.; Gu, J.-Y.; Shi, Z.-J. Palladium-Catalyzed Direct Annulation of Benzoic Acids with Phenols to Synthesize Dibenzopyranones. *Org. Lett.* **2017**, *19*, 1326–1329. (f) Wang, D.-Y.; Guo, S.-H.; Pan, G.-F.; Zhu, X.-Q.; Gao, Y.-R.; Wang, Y.-Q. Direct Dehydrogenative Arylation of Benzaldehydes with Arenes Using Transient Directing Groups. *Org. Lett.* **2018**, *20*, 1794–1797.

(3) For selected examples on directed oxidative Ar–H/Ar–H homo-couplings, see: (a) Hull, K. L.; Lanni, E. L.; Sanford, M. S. Highly Regioselective Catalytic Oxidative Coupling Reactions: Synthetic and Mechanistic Investigations. *J. Am. Chem. Soc*. **2006**, *128*, 14047–14049. (b) Oi, S.; Sato, H.; Sugawara, S.; Inoue, Y. Nitrogen-Directed *ortho*-Selective Homocoupling of Aromatic Compounds Catalyzed by Ruthenium Complexes. *Org. Lett.* **2008**, *10*, 1823–1826. (c) Pintori, D. G.; Greaney, M. F. Oxidative C–H Homodimerization of Phenylacetamides. *Org. Lett.* **2011**, *13*, 5713–5715. (d) Grigorjeva, L.; Daugulis, O. Cobalt-Promoted Dimerization of Aminoquinoline Benzamides. *Org. Lett*. **2015**, *17*, 1204–1207. (e) Gong, H.; Zeng, H.; Zhou, F.; Li, C.-J. Rhodium(I)-Catalyzed Regiospecific Dimerization of Aromatic Acids: Two Direct C–H Bond Activations in Water. *Angew. Chem., Int. Ed*. **2015**, *54*, 5718–5721. (f) Kondapalli, V.; Yu, X.; Yamamoto, Y.; Bao, M. Synthesis of 5*H*-Dibenzo[*c,e*]azepine-5,7(6*H*)-diones from Benzamides via Palladium-Catalyzed Double C–H Bond Activation. *J. Org. Chem.* **2017**, *82*, 2288–2293. (g) For a report referring some isolated examples of cross-coupling reactions, see: Zhang, C.; Rao, Y. Weak Coordination Promoted Regioselective Oxidative Coupling Reaction for 2,2'-Difunctional Biaryl Synthesis in Hexafluoro-2-propanol. *Org. Lett*. **2015**, *17*, 4456–4459.

(4) For examples on oxidative cross-couplings between directing group-containing arenes, see: (a) Zhang, X.-S.; Zhang, Y.-F.; Li, Z.-W.; Luo, F.-X.; Shi, Z.-J. Synthesis of Dibenzo[*c,e*]oxepin-5(7*H*)-ones from Benzyl Thioethers and Carboxylic Acids: Rhodium-Catalyzed Double C–H Activation Controlled by Different Directing Groups. *Angew. Chem., Int. Ed.* **2015**, *54*, 5478–5482. (b) Du, C.; Li, P.-X.; Zhu, X.; Suo, J.-F.; Niu, J.-L.; Song, M.-P. Mixed Directing-Group Strategy: Oxidative C–H/C–H Bond Arylation of Unactivated Arenes by Cobalt Catalysis. *Angew. Chem., Int. Ed.* **2016**, *55*, 13571–13575. (c) Zhang, C.; Li, T.; Wang, L.; Rao, Y. Synthesis of Diverse Heterocycles *via* One-Pot Cascade Cross-Dehydrogenative-Coupling (CDC)/Cyclization Reaction. *Org. Chem. Front.* **2017**, *4*, 386–391. (d) Zhang, C.; Song, Y.; Sang, Z.; Zhan, L.; Rao, Y. Mixing *O*-Containing and *N*-Containing Directing Groups for C–H Activation: A Strategy for the Synthesis of Highly Functionalized 2,2'-Biaryls. *J. Org. Chem.* **2018**, *83*, 2582–2591. (e) Mei, C.; Lu, W. Palladium(II)-Catalyzed Oxidative Homo- and Cross-Coupling of Aryl *ortho*-sp^2C–H Bonds of Anilides at Room Temperature. *J. Org. Chem.* **2018**, *83*, 4812–4823.

(5) (a) Bringmann, G.; Günther, C.; Ochse, M.; Schupp, O.; Tasler, S. Biaryls in Nature: A Multi-Facetted Class of Stereochemically, Biosynthetically, and Pharmacologically Intriguing Secondary Metabolites. *Prog. Chem. Org. Nat. Prod.* **2001**, *82*, 1–249. (b) Bringmann, G.; Mortimer, A. J. P.; Keller, P. A.; Gresser, M. J.; Garner, J.; Breuning, M. Atroposelective Synthesis of Axially Chiral Biaryl Compounds. *Angew. Chem., Int. Ed.* **2005**, *44*, 5384–5427. (c) Bringmann, G.; Gulder, T.; Gulder, T. A. M.; Breuning, M. Atroposelective Total Synthesis of Axially Chiral Biaryl Natural Products. *Chem. Rev.* **2011**, *111*, 563–639. (d) Wencel-Delord, J.; Panossian, A.; Leroux, F. R.; Colobert, F. Recent Advances and New Concepts for the Synthesis of Axially Stereoenriched Biaryls. *Chem. Soc. Rev.* **2015**, *44*, 3418–3430.

(6) (a) Höller, U.; König, G. M.; Wright, A. D. A New Tyrosine Kinase Inhibitor from a Marine Isolate of *Ulocladium botrytis* and New Metabolites from the Marine Fungi *Asteromyces cruciatus* and *Varicosporina ramulosa*. *Eur. J. Org. Chem.* **1999**, 2949–2955. (b) Yang, M.; Wu, J.; Cheng, F.; Zhou, Y. Complete Assignments of ^{1}H and ^{13}C NMR Data for Seven Arylnaphthalide Lignans from *Justicia procumbens*. *Magn. Reson. Chem.* **2006**, *44*, 727–730. (c) Shi, S.; Zhang, Y.; Huang, K.; Liu, S.; Zhao, Y. Application of Preparative High-Speed Counter-Current Chromatography for Separation and Purification of Lignans from *Taraxacum mongolicum*. *Food Chem.* **2008**, *108*, 402–406. (d) Zhou, Q.; Fu, Y.-H.; Zhang, Y.-Q.; Wu, S.-Y.; Song, X.-P.; Cao, C.-K.; Xu, W.; Chen, G.-Y. Fissitungfines A and B, Two Novel Aporphine Related Alkaloids from *Fissistigma tungfangense*. *Tetrahedron Lett.* **2016**, *57*, 4162–4164. (e) Weinberg, M. A. RES-529: A PI3K/AKT/mTOR Pathway Inhibitor that Dissociates the mTORC1 and mTORC2 Complexes. *Anti-Cancer Drugs* **2016**, *27*, 475–487.

(7) Shi, Y.; Zhang, L.; Lan, J.; Zhang, M.; Zhou, F.; Wei, W.; You, J. Oxidative C–H/C–H Cross-Coupling Reactions between *N*-Acylanilines and Benzamides Enabled by a Cp*-Free $RhCl_3$/TFA Catalytic System. *Angew. Chem., Int. Ed.* **2018**, *57*, 9108–9112.

(8) An example on Ru(II)-catalyzed acyloxylation of 2-aryloxypyridines, see: Raghuvanshi, K.; Rauch, K.; Ackermann, L. Ruthenium(II)-Catalyzed C–H Acyloxylation of Phenols with Removable Auxiliary. *Chem. - Eur. J.* **2015**, *21*, 1790–1794.

(9) (a) Campbell, A. N.; Stahl, S. S. Overcoming the "Oxidant Problem": Strategies to Use O_2 as the Oxidant in Organometallic C–H Oxidation Reactions Catalyzed by Pd (and Cu). *Acc. Chem. Res.* **2012**, *45*, 851–863. (b) Shi, Z.; Zhang, C.; Tang, C.; Jiao, N. Recent Advances in Transition-Metal Catalyzed Reactions Using Molecular Oxygen as the Oxidant. *Chem. Soc. Rev.* **2012**, *41*, 3381–3430. (c) Allen, S. E.; Walvoord, R. R.; Padilla-Salinas, R.; Kozlowski, M. C. Aerobic Copper-Catalyzed Organic Reactions. *Chem. Rev.* **2013**, *113*, 6234–6458. (d) Gulzar, N.; Schweitzer-Chaput, B.; Klussmann, M. Oxidative Coupling Reactions for the Functionalisation of C–H Bonds Using Oxygen. *Catal. Sci. Technol.* **2014**, *4*, 2778–2796. (e) Muthusamy, S., Kumarswamyreddy, N., Kesavan, V., Chandrasekaran, S. Recent

Advances in Aerobic Oxidation with Ruthenium Catalysts. *Tetrahedron Lett.* **2016**, *57*, 5551–5559.

(10) Zhao, Y.; He, Z.; Li, S.; Tang, J.; Gao, G.; Lan, J.; You, An Air-Stable Half-Sandwich Ru^{II} Complex as an Efficient Catalyst for [3+2] Annulation of 2-Arylcyclo-2-enones with Alkynes. *Chem. Commun.* **2016**, *52*, 4613-4616.

(11) For more details about the optimization of reaction conditions, see the Supporting Information.

(12) (a) Xue, Q.; Hopkins, B.; Perruzzi, C.; Udayakumar, D.; Sherris, D.; Benjamin, L. E. Palomid 529, a Novel Small-Molecule Drug, Is a TORC1/TORC2 Inhibitor That Reduces Tumor Growth, Tumor Angiogenesis, and Vascular Permeability. *Cancer Res.* **2008**, *68*, 9551–9557. (b) Diaz, R.; Nguewa, P. A.; Diaz-Gonzalez, J. A.; Hamel, E.; Gonzalez-Moreno, O.; Catena, R.; Serrano, D.; Redrado, M.; Sherris, D.; Calvo, A. The Novel Akt Inhibitor Palomid 529 (P529) Enhances the Effect of Radiotherapy in Prostate Cancer. *Br. J. Cancer* **2009**, *100*, 932–940. (c) Dalal, M.; Jacobs-El, N.; Nicholson, B.; Tuo, J.; Chew, E.; Chan, C.-C.; Nussenblatt, R.; Ferris, F.; Meyerle, C. Subconjunctival Palomid 529 in the Treatment of Neovascular Age-Related Macular Degeneration. *Graefes Arch. Clin. Exp. Ophthalmol.* **2013**, *251*, 2705–2709.

(13) Sherris, D. Compositions and Methods to Treat Skin Diseases Characterized by Cellular Proliferation and Angiogenesis. U.S. Patent 2006/0257337 A1, Nov 16, 2006.

(14) When a stoichiometric amount of $[Ru(p\text{-cymene})(MeCN)_3](SbF_6)_2$ was used, no desired product was detected, probably because the coordinated acetonitrile inhibited the coordination of the substrates to the ruthenium center.

(15) (a) Peverati, R.; Truhlar, D. G. Screened-Exchange Density Functionals with Broad Accuracy for Chemistry and Solid-State Physics. *Phys. Chem. Chem. Phys.* **2012**, *14*, 16187–16191. (b) Peverati, R.; Truhlar, D. G. M11-L: A Local Density Functional that Provides Improved Accuracy for Electronic Structure Calculations in Chemistry and Physics. *J. Phys. Chem. Lett.* **2012**, *3*, 117–124. (c) Zhao, Y.; Ng, H. T.; Peverati, R.; Truhlar, D. G. Benchmark Database for Ylidic Bond Dissociation Energies and Its Use for Assessments of Electronic Structure Methods. *J. Chem. Theory Comput.* **2012**, *8*, 2824–2834. (d) Yu, Z.; Lan, Y. Mechanism of Rhodium-Catalyzed Carbon–Silicon Bond Cleavage for the Synthesis of Benzosilole Derivatives: A Computational Study. *J. Org. Chem*. **2013**, *78*, 11501–11507.(e) Zhu, L.; Qi, X.; Lan, Y. Rhodium-Catalyzed Hetero-(5 + 2) Cycloaddition of Vinylaziridines and Alkynes: A Theoretical View of the Mechanism and Chirality Transfer. *Organometallics* **2016**, *35*, 771–777.

(16) (a) Lee, C.; Yang, W.; Parr, R. G. Development of the Colic-Salvetti Correlation-Energy Formula into a Functional of the Electron Density. *Phys. Rev. B* **1988**, *37*, 785–789. (b) Becke, A. D. Density-Functional Thermochemistry. III. The Role of Exact Exchange. *J. Chem. Phys.* **1993**, *98*, 5648–5652.

(17) For more computational details, see the Supporting Information.

(18) Only 27% NMR yield of homo-coupled product **1aa** was obtained when **1a** was used as substrate alone under the standard conditions. See the Supporting Information for more details.

(19) Only 15% NMR yield of homo-coupled product **2aa** was obtained when **2a** was used as substrate alone under the standard conditions. See the Supporting Information for more details.

(20) (a) Tauchert, M. E.; Incarvito, C. D.; Rheingold, A. L.; Bergman, R. G.; Ellman, J. A. Mechanism of the Rhodium(III)-Catalyzed Arylation of Imines via C–H Bond Functionalization: Inhibition by Substrate. *J. Am. Chem. Soc.* **2012**, *134*, 1482–1485; (b) Park, S. H.; Kwak, J.; Shin, K.; Ryu, J.; Park, Y.; Chang, S. Mechanistic Studies of the Rhodium-Catalyzed Direct C–H Amination Reaction Using Azides as the Nitrogen Source. *J. Am. Chem. Soc.* **2014**, *136*, 2492–2502; (c) Park, Y.; Park, K. T.; Kim, J. G.; Chang, S. Mechanistic Studies on the Rh(III)-Mediated Amido Transfer Process Leading to Robust C–H Amination with a New Type of Amidating Reagent. *J. Am. Chem. Soc.* **2015**, *137*, 4534–4542.

(21) (a) Ferrer Flegeau, E.; Bruneau, C.; Dixneuf, P. H.; Jutand, A. Autocatalysis for C–H Bond Activation by Ruthenium(II) Complexes in Catalytic Arylation of Functional Arenes. *J. Am. Chem. Soc.* **2011**, *133*, 10161–10170. (b) Shang, M.; Zeng, S.-H.; Sun, S.-Z.; Dai, H.-X.; Yu, J.-Q. Ru(II)-Catalyzed *ortho*-C–H Amination of Arenes and Heteroarenes at Room Temperature. *Org. Lett.* **2013**, *15*, 5286–5289. (c) Yang, X.; Sun, Y.; Chen, Z.; Rao, Y. A General Approach towards Catechol and Pyrogallol through Ruthenium- and Palladium-Catalyzed C–H Hydroxylation by Weak Coordination. *Adv. Synth. Catal.* **2014**, *356*, 1625–1630. (d) Nareddy, P.; Jordan, F.; Szostak, M. Recent Developments in Ruthenium-Catalyzed C–H Arylation: Array of Mechanistic Manifolds. *ACS Catal.* **2017**, *7*, 5721–5745.

Table of Content